# Passive Millimeter Wave Imaging Using a Distributed Aperture and Optical Upconversion

Thomas E. Dillon[a], Christopher A. Schuetz[a], Richard D. Martin[a], Shuoyuan Shi[b], Daniel G. Mackrides[a], and Dennis W. Prather[b*]

[a] Phase Sensitive Innovations Inc., 51 East Main Street, Suite 201, Newark, DE 19711 USA
[b] Department of Electrical and Computer Engineering, University of Delaware, 140 Evans Hall, Newark, DE 19716 USA

## ABSTRACT

We report on our initial results of passive, real-time imaging in the Q-band using a distributed aperture and optical upconversion. The basis of operation is collection of incident mmW radiation by the distributed aperture, as embodied by an array of horn antennas, which is then amplified and upconverted to optical frequencies using commercially available electro-optic modulators. The non-linear mixing of the modulators creates sidebands containing the mmW signal with both amplitude and phase preserved. These signals are relaunched in the optical domain with a homothetic mapping of the antenna array. The optical carrier is stripped via dielectric stack filters and imagery is synthesized from the sidebands using the Fourier transform properties of a simple lens. This imagery is collected using a standard near-infrared camera with post-processing to enhance the signal of interest and reduce noise. Details of operation and presentation of sample imagery is presented herein.

**Keywords:** passive millimeter wave imaging, distributed aperture imaging, optical upconversion

## 1. INTRODUCTION

Millimeter-wave radiation lies in the electromagnetic spectrum between microwave and terahertz frequencies. All physical objects emit thermal radiation according to the Rayleigh-Jeans law. However, terrestrial objects near room temperature emit roughly eight orders of magnitude lower irradiance in the mmW spectrum as compared to the optical spectrum. This necessitates very sensitive receivers for imaging in this regime with associated technological challenges to make mmW imaging feasible. On the other hand, there is considerable interest in using this region of the spectrum due to the fact that mmW radiation can penetrate thin dielectric materials as well as atmospheric obscurants [1]. As a result, potential applications include stand-off threat detection, portal screening, aerial reconnaissance, persistent surveillance, and situational awareness in degraded visual environments [2-6].

Millimetre Wave and Terahertz Sensors and Technology III, edited by Keith A. Krapels, Neil A. Salmon, Proc. of SPIE Vol. 7837, 78370H · © 2010 SPIE · CCC code: 0277-786X/10/$18 · doi: 10.1117/12.865081



http://dx.doi.org/10.1117/12.865081

* dprather@ee.udel.edu

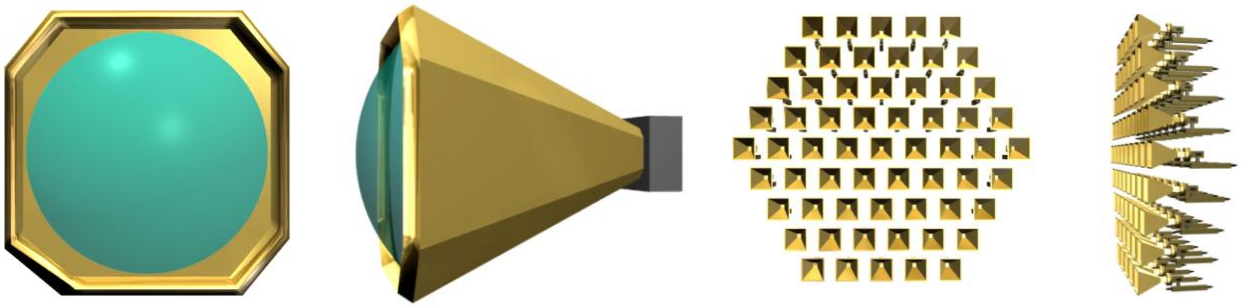

Figure 1: Three-dimensional form factor for a conventional imager relying on refractive optics and a focal plane array (front and side view, left) and an essentially two-dimensional form-factor for a distributed aperture imager with comparable aperture size and hence resolution capability (front and side view, right).

Because of the relatively long wavelengths of mmW radiation as compared to those in the optical spectrum, large aperture sizes are needed to achieve sufficient resolution for most applications of interest. For conventional imaging systems consisting of refractive optics and a focal plane array, increasing aperture size results in volumetric scaling of the imager with commensurate weight increase. In contrast, a distributed aperture imaging system is essentially two-dimensional in nature and can achieve effectively large apertures, thus providing the requisite resolution in a smaller form factor, as illustrated in Figure 1. In comparing the two approaches in this figure it should be pointed out that additional hardware is required for processing the collected signals; that is, only the front-end of the systems is represented here. However, back-end hardware for the distributed aperture imager potentially can be made small and lightweight, thus maintaining its advantage over the conventional imager approach.

## 2. IMAGER OVERVIEW

A prototype imager was constructed as shown in Figure 2. At this point, no effort was made to minimize size, weight, or power requirements; the main objective was to prove the validity of the distributed aperture imaging approach. Nonetheless, this prototype also serves as a test bed for new components as they are developed to improve system performance. To this end, we are currently working on moving the system to W-band operation with in-house developed modulators, integrating the modulators with low-noise amplifiers and antennas into compact sensor nodes, significantly reducing the size of the optical processor, eliminating the bulky and power-hungry EDFAs by increasing front-end gain, and replacing the COTS FPGA-based phase control system with more compact custom electronics also developed in-house. Significant milestones associated with this development are the move to W-band operation, which will increase the resolution performance for a fixed aperture size, the move to an aperiodic antenna array with associated aperiodic optics to eliminate aliasing in the imagery and thus increase the field of view, and an increase in the number of sensor nodes to increase diffraction efficiency and thus improve noise performance of the imager.

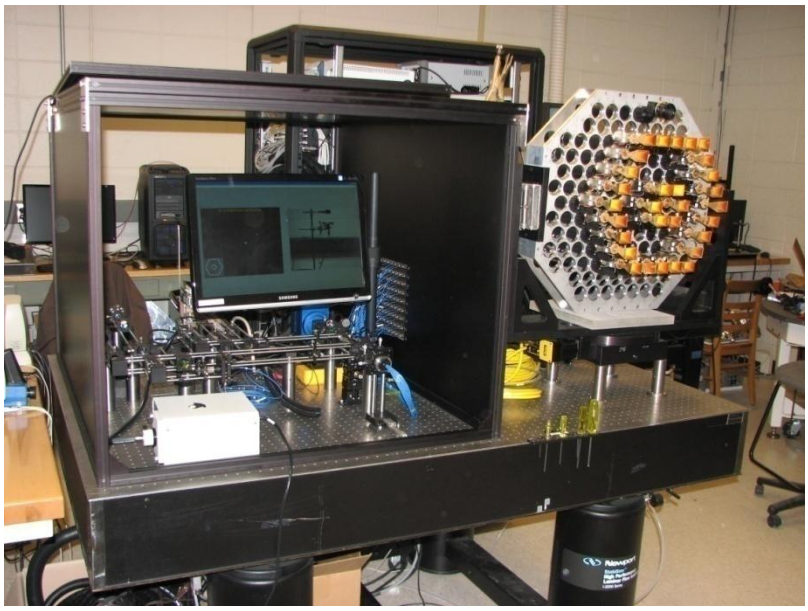

Figure 2: Prototype distributed aperture imager. RF front-end is shown at right, optical processing is performed in hardware at left, and supporting hardware is rack-mounted in the background.

A schematic overview of the imaging system is presented in Figure 3. An optical feed consisting of a distributed feedback (DFB) laser operating at telecom frequencies is amplified by an erbium doped fiber amplifier (EDFA) to provide sufficient optical power. This optical power is supplied to a 1x32 splitter network, which then feeds each of the 30 sensor nodes. The nodes are arranged in a dual ring hexagonal configuration with fixed pitch. As shown in Figure 4, each sensor node consists of a pyramidal horn antenna connected to an integrated RF module and phase modulator. Inside each module are two stages of low-noise amplifiers and a p-i-n switch. This switch is used to alternately sample the antenna temperature and a 50Ω load noise temperature, which is used as a reference level in a scheme similar to Dicke switching, as will be discussed later. The RF module is connected to the optical modulator via a waveguide to coax converter. Optical power from the splitter network is supplied to each modulator and the mmW signal is introduced into sidebands separated from the carrier at multiples of the RF operating frequency of the imager. Further discussion of the optical upconversion scheme may be found in a prior publication [7].

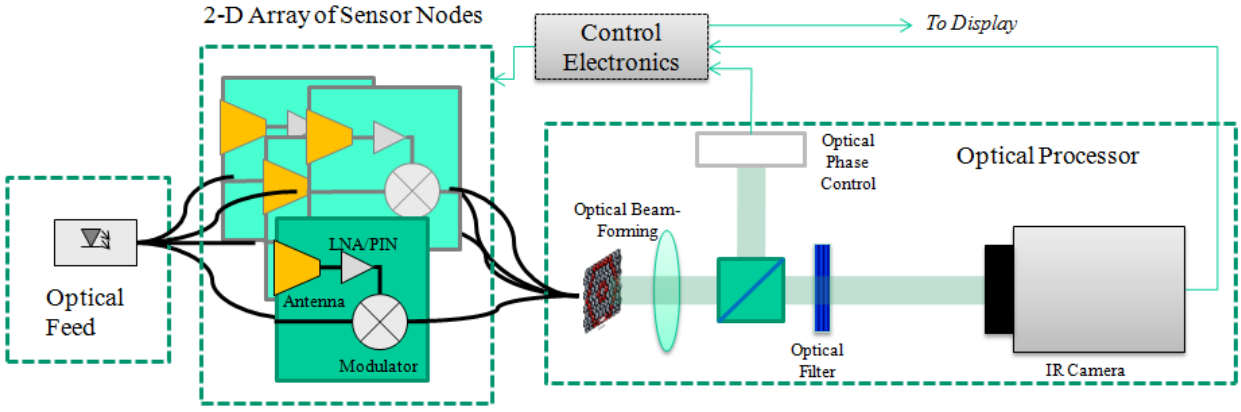


Figure 3: Schematic overview of the prototype imaging system. The system consists of an optical feed, an array of sensor nodes, an optical processor, and control electronics to maintain phase control of the individual nodes.

After upconversion of the mmW radiation onto sidebands of the optical carrier, these signals are routed via optical fibers and relaunched into free space using a two-dimensional fiber array that matches the geometry of the antenna array. The fiber array is mated to a microlens array such that each beamlet is collimated; these collimated beams pass through a cascade of dielectric stack filters such that the carrier and extraneous sidebands are adequately suppressed. The remaining optical power represents the mmW signal of interest. The fiber array is located one focal length away from a simple lens such that an optical Fourier transform is performed, which synthesizes an infrared image of the scene sampled by the antenna array in the mmW spectrum on a standard NIR focal plane array (FPA) also one focal length away from the lens. A detailed discussion of the imager optical configuration was published previously [8].

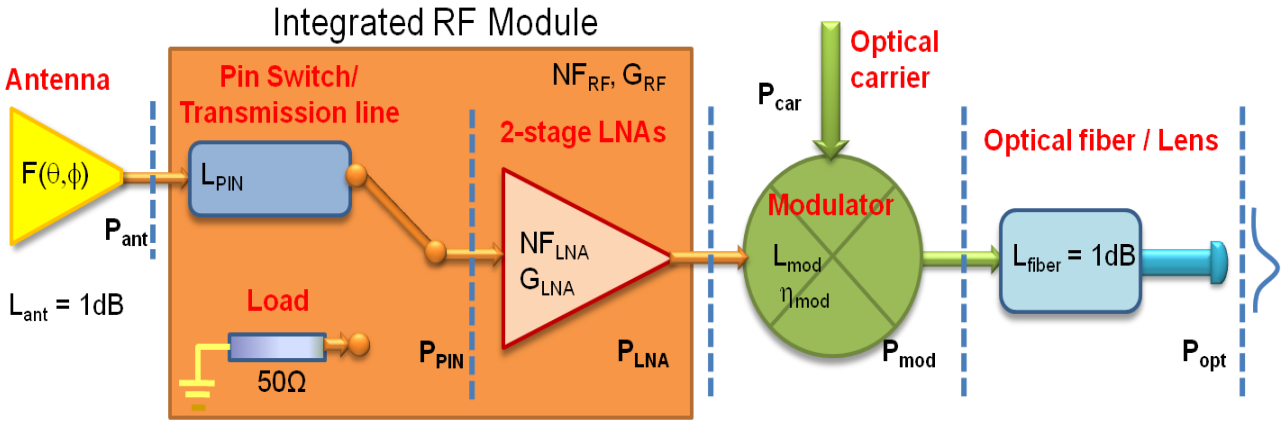


Figure 4: Front-end of the mmW imager, consisting of an antenna array, integrated RF module, and phase modulator.

## 3. IMAGER CALIBRATION

In order to synthesize the imagery in the optical domain, it is necessary to maintain control of the phase of each individual imager channel. Because of thermal and vibrational coupling into the optical fibers, the phase relationship between channels cannot be maintained without some form of active compensation. This is achieved by sampling the phase of each channel within the optical processor and using this information as feedback to the sensor nodes. Beyond maintaining the phase of each channel, a phase offset can be added as well. This allows, for example, focusing of the imager for a particular range by adding quadratic phase across the antenna array or steering of the FOV by adding a linear phase across the antenna array.

Because of variations is phase due to the transfer characteristics of the RF modules and differences in optical path length within each channel, the phase relationship between channels must be calibrated in order to produce the desired imagery. As such, one of the channels is chosen as a phase reference and power applied to its sensor node. Another channel is selected to calibrate its phase relative to the reference and power is then applied to its sensor node. With these two channels powered up, a fringe pattern becomes visible as imaged on the FPA; this is illustrated in Figure 5. The fringe pattern can be shifted by adjusting the phase of the channel being calibrated. For our purpose, we adjust the phase on the channel such that a fringe peak is located at the center of the FPA. This procedure is repeated for each of the remaining channels, aligning each of the fringe patterns to produce a peak at the same location for each channel. Subsequently, when all channels are powered on and phase aligned, the optical point spread function (PSF) becomes apparent on the FPA.

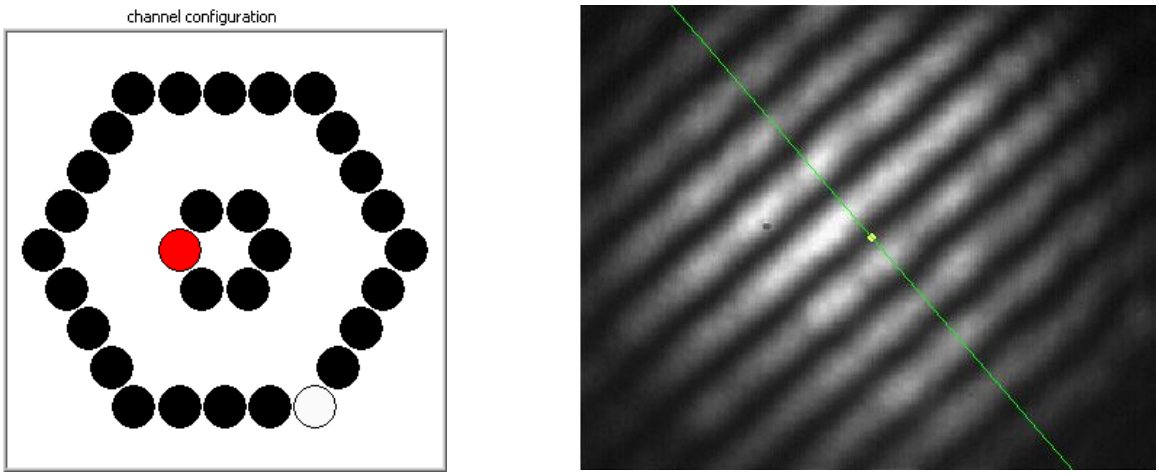


Figure 5. Phase calibration between channels (left) is accomplished by choosing a reference channel (shown in red) and adjusting the phase on the channel being calibrated (shown in white) such that the image fringe pattern (right) produces a peak at the center of the FPA. This procedure is repeated for each of the remaining channels relative to the selected reference channel.

There is another aspect of the imager calibration to be considered here: the shift in the fringe pattern is frequency dependent. Because the imager operates over a finite bandwidth, the resulting pattern observed is actually the summation of the fringe patterns resulting over this bandwidth. If the RF bandwidth is large and the optical path lengths of each of the channels are not maintained within the associated coherence length, a phenomenon known as fringe washing results. Some means of maintaining optical path lengths within the RF coherence length is required to maximize fringe visibility, since this directly affects the contrast available in the synthesized images.

Because the fiber lengths are fixed, an alternate method to adjust for maximum fringe visibility is needed. We found that by adjusting the positions of each individual sensor node in the array orthogonal to the array mounting plate a time advance (or delay) could be produced such that the fringe position remains independent of frequency. As a result, the fringe visibility was optimized through adjustment of the sensor node positions, as shown in Figure 6.

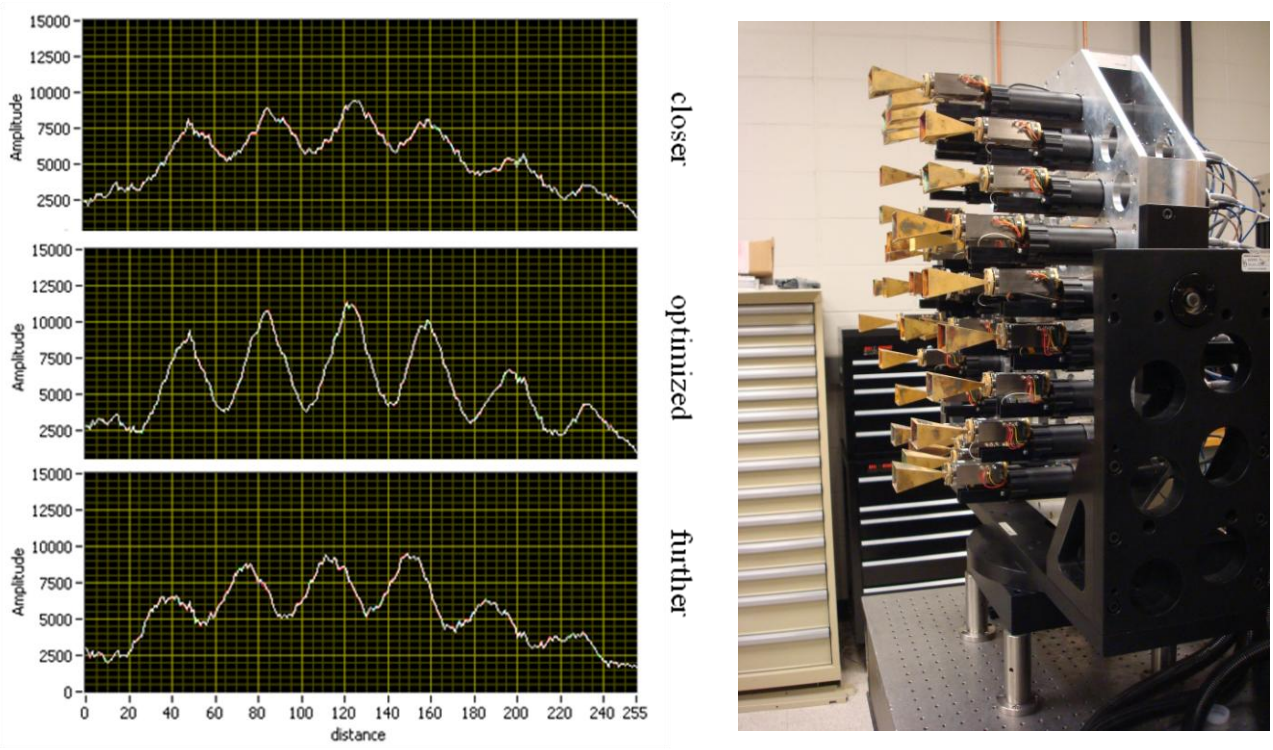


Figure 6. The fringe visibility (left) is optimized by adjusting the position of each individual sensor node orthogonal to the array mounting plate (right).

## 4. SYSTEM OPERATION

Once the imager has been calibrated in terms of phase offsets for each channel as well as sensor node positions within the array mounting plate, the system is ready for image acquisition. To produce a suitable target for imaging, we constructed the apparatus shown in Figure 7. This consists of an absorber soaked in liquid nitrogen, whose temperature brightness is reflected from a metal plate positioned at 45º and selectively masked by an absorber at room temperature with cut-outs. In this way, a passive target with a temperature contrast comparable to that between terrestrial objects and cold sky is realized.

The steps involved in producing imagery from the raw collected signals is shown in Figure 8. The p-i-n switch in the RF module is alternated between sampling the antenna temperature and the noise temperature of the internal load. The NIR camera triggering is synchronized with the p-i-n switch and a frame of the FPA is collected for each of these alternate states. The load frame is subtracted from the antenna frame such that the load serves as a reference temperature. A number of such difference frames are collected and averaged. At first this procedure is performed with the imager staring at a room-temperature absorber to produce the bright frame. The bright frame is used in a later step to remove fixed pattern noise (FPN) from the gray frame, which will be defined next. The imager is aimed at the passive target of interest and a running first-in-last-out (FILO) buffered is maintained of desired size over which temporal averaging is performed; this results in the gray frame. Temporal averaging is used to reduce noise since the well size of the FPA can be filled faster than the required frame rate. The bright frame is subtracted from the gray frame to remove FPN and a spatial average is performed to further reduce noise in the image. This spatial averaging does not affect the final image resolution since the mmW scene is oversampled by the pixel size of the NIR FPA.

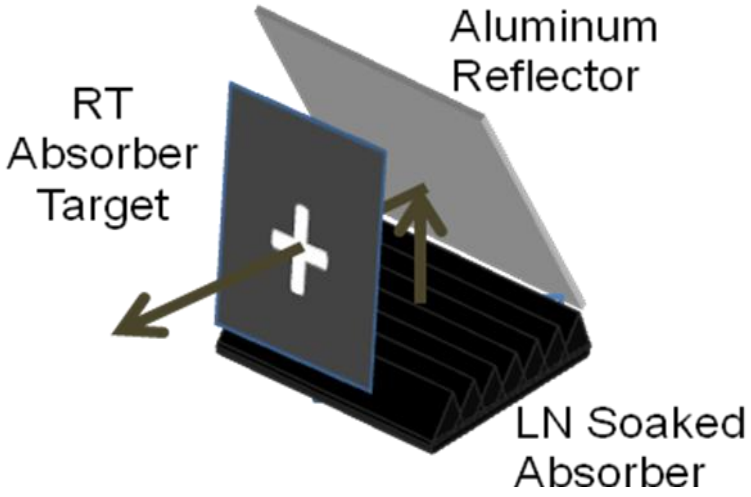


Figure 7. Construction of a passive target for use in evaluating imager operation.

We present results of image acquisition in Figure 9. Two targets were constructed for this experiment: a cross pattern and a line and space pattern. Visible images are presented along with the corresponding images from our mmW imager. Also shown in this figure are simulated images produced by a first-principles model accounting for all measured parameters of the system components including a comprehensive noise model. Good agreement between the experimental and simulated imagery is achieved.

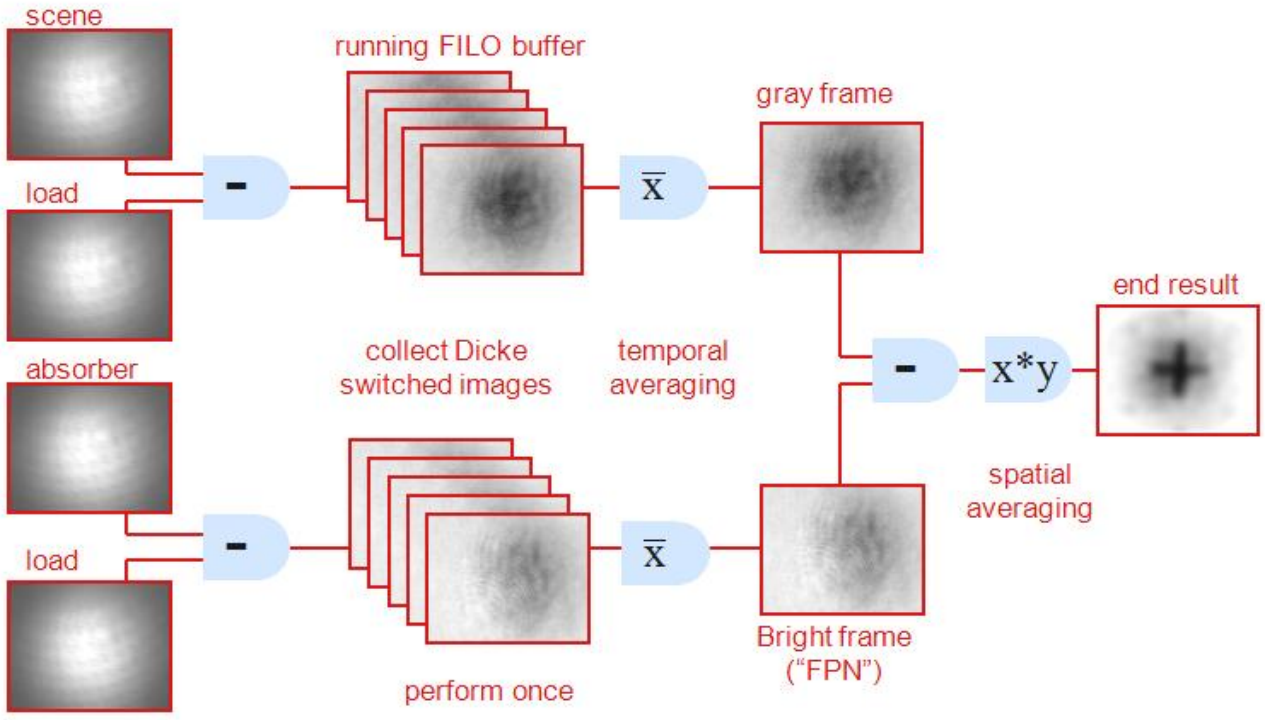


Figure 8: Steps involved in producing an image from the raw collected FPA frames. Details are presented in the text.

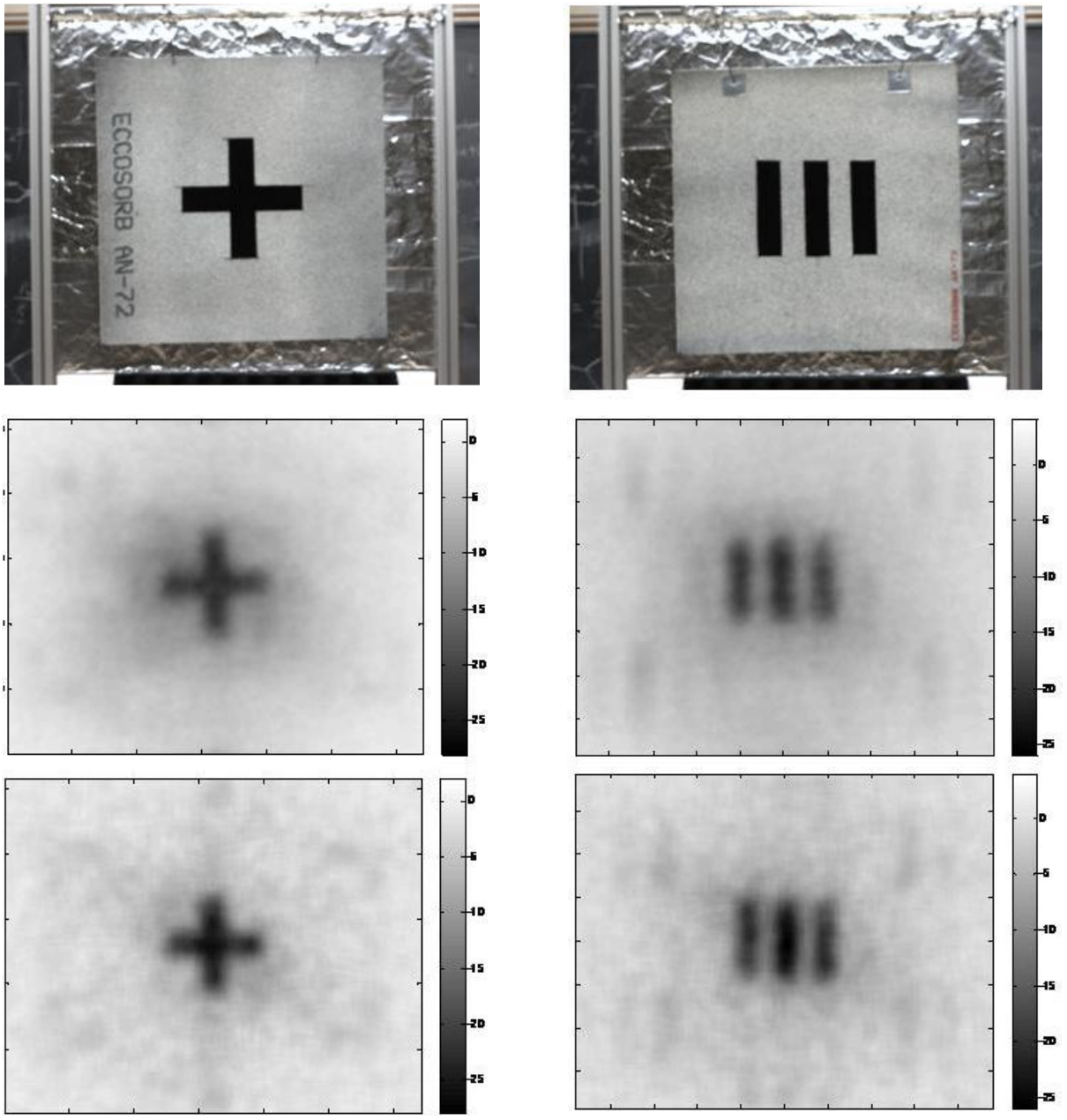


Figure 9: Visible, mmW, and simulated imagery (from top to bottom) for a cross pattern (left) and a bar pattern (right).

## 5. CONCLUSION

We have presented a passive millimeter wave imaging system utilizing a distributed aperture antenna array and optical upconversion. An overview of the system along with details of the system components were given. Also presented was a discussion of the calibration and operation of the imager. Extended source passive imagery was demonstrated and compared to simulated results with good agreement between the two. This imagery was collected at video frame rates.

## 6. ACKNOWLEDGMENTS

We would like to thank Dr. Elizabeth Twarog, Dr. Dave Dowgiallo, and Dr. Peter Gaiser of the Naval Research Laboratory and their colleagues as well as Dr. Michael Duncan at the Office of Naval Research - Information, Electronics, and Surveillance Division for providing technical oversight regarding various aspects of this work.

## 7. REFERENCES

[1] F. T. Ulaby, R. K. Moore, and A. K. Fung, Microwave Remote Sensing: Active and Passive, Vol. I -- Microwave Remote Sensing Fundamentals and Radiometry, Addison-Wesley, Reading, Massachusetts, 1981.

[2] D. M. Sheen, D. L. McMakin, and T. E. Hall, "Three-Dimensional Millimeter-Wave Imaging for Concealed Weapon Detection," *IEEE Transactions on Microwave Theory and Techniques*, Volume 49, pp. 1581-1592, 2001.

[3] L. Yujiri, M. Shoucri, and P. Moffa, "Passive Millimeter-Wave Imaging," *IEEE Microwave Magazine*, pp. 39-50, September 2003.

[4] Major D. W. Pendall, "Persistent Surveillance and Its Implication for the Common Operating Picture," *Military Review*, pp. 41-50, November-December 2005.

[5] S. Scheding, G. Brooker, R. Hennessy, M. Bishop, and A. Maclean, "Terrain Imaging and Perception using Millimetre Wave Radar," *Proc. 2002 Australasian Conference on Robotics and Automation*, pp. 60-65, 2002.

[6] C. A. Schuetz, E. L. Stein, Jr., J. Samluk, D. Mackrides, J. P. Wilson, R. D. Martin, T. E. Dillon, and D. W. Prather, "Studies of Millimeter Wave Phenomenology for Helicopter Brownout Mitigation," *Proceedings of SPIE*, Volume 7485, 2009.

[7] C. A. Schuetz, J. Murakowski, G. J. Schneider, and D. W. Prather, "Radiometric millimeter-wave detection via optical upconversion and carrier suppression," *IEEE Transactions on Microwave Theory and Techniques*, Volume 53, pp. 1732-1738, 2005.

[8] T. E. Dillon, C. A. Schuetz, R. D. Martin, E. L. Stein, Jr., J. P. Samluk, D. G. Mackrides, M. S. Mirotznik, and D. W. Prather, "Optical Configuration of an Upconverted Millimeter-Wave Distributed Apterture Imaging System," *Proceedings of SPIE*, Volume 7485, 2009.